A Cold Startup Strategy for Blind Adaptive M-PPM Equalization

Andrew G. Klein and Xinming Huang
Department of Electrical and Computer Engineering
Worcester Polytechnic Institute
Worcester, MA 01609
email: {klein,xhuang}@ece.wpi.edu

***Abstract*—We explore a blind strategy for cold-startup of an adaptive equalization structure suitable for use with pulse-position modulated (PPM) signals. In particular, we explore a combination of two recent results: [1] and [2]. In [1], a novel block symbol-rate equalizer was proposed where critically-sampled PPM systems can perfectly equalizer an FIR channel. Another recent result [2] proposed the only known blind adaptive algorithm for adapting a conventional chip-rate equalizer for PPM signaling. We explore the behavior of the blind adaptive algorithm when one of the key assumptions necessary for global convergence is violated, and show that even without this assumption it is nonetheless a good candidate for cold-startup of the block equalizer structure.**

I. Introduction

Pulse-position modulation (PPM) is a digital modulation format that has seen considerable attention over the past several decades, particularly in applications which require high energy efficiency. Traditional uses of PPM have been in situations with little or no intersymbol interference (ISI), and thus until recently there had been little motivation to explore equalization of such signals to the extent that equalization has been explored for linearly modulated signals. In the 1980's and early 1990's, much attention was given to M-ary PPM for its use on optical and nondirected infared channels (see for example [3] and references therein). More recently, PPM has been considered by the ultra-wideband (UWB) community for so-called impulse radios [4]. While several studies of ISI compensation for PPM were conducted a decade ago in the optical communications context [3][5], the recent interest in PPM for use in high-speed UWB communication over short range has revived interest in equalization of PPM signals [1][2].

In the absense of ISI, PPM is appealing because it permits the use of relatively simple non-coherent detection schemes [6]. The multipath spread of a typical UWB indoor channel may be as large as several hundred nanoseconds [4], however, which results in significant ISI at the high data rates for which UWB is intended. While the optimum PPM detector in ISI is the maximum likelihood sequence estimator (MLSE) which was investigated in [7], its complexity is usually too high for practical implementation, and thus suboptimal schemes are preferred in practice.

In this paper, we explore a combination of two recent results: [1] and [2]. In [1], it was shown that the structure of the PPM signal has properties that permit perfect equalization with a finite-length block symbol-rate equalizer. This contradicts conventional wisdom about equalization for more traditional modulations like pulse amplitude modulation (PAM), since for PAM systems it is well-known that a finite-length linear equalizer cannot perfectly invert an FIR channel unless oversampling is employed [8]. By exploiting the structure of the PPM signal, it was shown that critically-sampled PPM systems enable perfect linear equalization — no oversampling is required if a particular block equalizer structure is employed. The scheme in [1] requires channel knowledge or that training symbols are sent from the transmitter. However, another recent result [2] proposed a *blind* adaptive algorithm for adapting a conventional scalar chip-rate equalizer. The algorithm in [2] is based on the third-moment of the PPM signal, and is shown to be globally convergent under some simplifying assumptions. We will show how to employ the blind algorithm in [2] for cold startup of the block equalizer of [1], and demonstrate that it leads to an open-eye equalizer. One of the simplifying assumptions in [2] is that the PPM alphabet size, M, tends toward infinity. Thus, we will additionally explore the behavior of the blind algorithm when M is finite.

II. Block Equalizer for Complete ISI Removal

A. System Model

M-ary PPM is an orthogonal transmission scheme where a symbol consists of M *chips*, only one of which is non-zero. PPM can be thought of as a block coding scheme where information is conveyed by the location of the non-zero sample within the block of M chips. Thus, the symbol alphabet comprises the M columns of the identity matrix $\boldsymbol{I}_M$. We assume that adjacent symbols are sent with no guard time between them, and as in [5] we assume a discrete-time model where each chip is sampled once. We denote the symbol transmitted at time n by $\boldsymbol{x}[n] \in \{\boldsymbol{e}_0, \ldots, \boldsymbol{e}_{M-1}\}$. While we assume that symbols are i.i.d., the resulting chip rate sequence is certainly not, though it is cyclostationary with period M. Clearly, the PPM source is not zero-mean, and $\boldsymbol{\mu}_x \triangleq E[\boldsymbol{x}[n]] = \frac{1}{M}\mathbf{1}_{M\times 1}$.

The system model for the transmitter, channel, and equalizer/receiver is shown in Fig. 1. The i.i.d. M-ary PPM symbols $\boldsymbol{x}[n]$ are transmitted serially through a causal linear time-invariant FIR channel of length N_h with impulse response

$\boldsymbol{h} = [h[0] \ \ldots \ h[N_h - 1]]^\top$ and additive white Gaussian noise $\boldsymbol{w}[n]$ where each sample has variance σ_w^2 assumed to be uncorrelated with the data. A vector model for the length

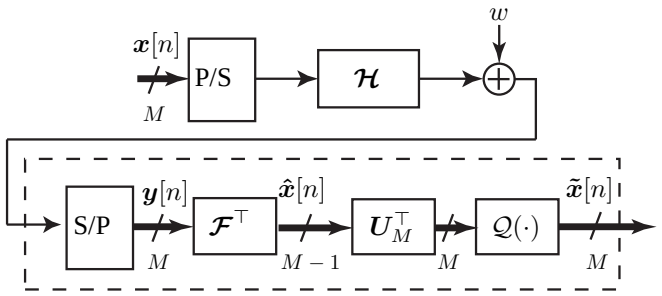

Fig. 1. Block Equalizer System Model

N_f received vector at time n is then

$$\bar{\boldsymbol{y}}[n] = \boldsymbol{\mathcal{H}}\bar{\boldsymbol{x}}[n] + \bar{\boldsymbol{w}}[n] \tag{1}$$

where $\bar{\boldsymbol{y}}[n] \in \mathbb{R}^{N_f}$ is the stacked vector of received symbols, $N_c \triangleq N_f + N_h - 1$ is the combined length of the channel and feedforward equalizer, $\boldsymbol{\mathcal{H}} \in \mathbb{R}^{N_f \times N_c}$ is the Tœplitz channel convolution matrix defined as $[\boldsymbol{\mathcal{H}}]_{i,j} = h[j-i]$, $\bar{\boldsymbol{x}}[n] \in \mathbb{R}^{N_c}$ is the serialized vector of transmitted PPM symbols, and $\bar{\boldsymbol{w}}[n] \in \mathbb{R}^{N_f}$ is the AWGN. Note that, as in [5], our receiver employs coherent reception in the sense that it preserves the polarity of the received signal (as opposed to simple energy detection).

To exploit the cyclostationary source statistics, we consider a symbol-rate *block* equalizer (as opposed to a chip-rate scalar equalizer). Since this block equalizer can alternatively be thought of as a single periodically time-varying chip rate equalizer, it has equivalent computational complexity to a traditional single scalar equalizer operating at the chip rate. Thus, we could filter the received signal with a block feedforward filter $\boldsymbol{\mathcal{F}} \in \mathbb{R}^{N_f \times M}$ where each column of $\mathcal{F}$ effectively equalizes each of the M polyphases of a PPM symbol. However, as shown in [1], a PPM signal can be projected into a subspace of reduced dimension, i.e. from dimension M to dimension $M-1$, without changing the Euclidean distance properties of the signal. Thus, instead of equalizing a given symbol in the traditional sense, we consider a reduced filter $\boldsymbol{\mathcal{F}} \in \mathbb{R}^{N_f \times M-1}$ which performs equalization in the signal subspace of dimension $M-1$. Then, before making decisions, we can re-project the signal back into the traditional PPM signal set of dimension M with a projection matrix $\boldsymbol{U}_M^\top$, to be described below.

The decision device that we employ here is the minimum Euclidean distance detector, which simply amounts to choosing the largest element of the length M received vector [9]. While we have chosen this decision device for its simplicity and low latency, we note that it is the optimal (i.e. maximum likelihood) PPM decision device in the memoryless AWGN channel in the absence of ISI. We let $\mathcal{Q}(\cdot)$ denote the nonlinear decision-making operation, so that the decision device output can be written $\hat{\boldsymbol{x}}[n] = \mathcal{Q}(\boldsymbol{U}_M^\top \tilde{\boldsymbol{x}}[n])$ where the function $\mathcal{Q}(\cdot)$ is defined as

$$\mathcal{Q}(\boldsymbol{U}_M^\top \tilde{\boldsymbol{x}}[n]) = \boldsymbol{e}_i \tag{2}$$

with i being the index of the largest element in the vector $\boldsymbol{U}_M^\top \tilde{\boldsymbol{x}}[n]$.

B. Equalizer Coefficients for Complete ISI Removal

We now consider the conditions that permit a feedforward equalizer to perfectly remove the ISI (i.e. the "zero-forcing" equalizer). For more traditional modulations like pulse amplitude modulation (PAM), it is well-known that a finite-length linear equalizer cannot perfectly invert an FIR channel unless oversampling or multiple sensors are employed [8]. It is perhaps a bit surprising that, even without oversampling, all ISI can be removed in PPM systems with only a finite-length feedforward filter. Since the decision device is invariant to DC offsets (i.e. adding some constant to all chips of a particular symbol), we are willing to accept an equalizer that introduces arbitrary DC offsets to a given symbol if it reduces the the number of parameters in the equalizer. Because of this extra degree of freedom, we can formulate the equalizer design criterion in a space of reduced dimension so that the equalizer operates only in the relevent subspace. First, we present a key lemma from [1] which serves to motivate this approach:

Lemma 1.
The PPM minimum Euclidean distance detector function $\mathcal{Q}(\cdot)$ defined in (2) satisfies

$$\mathcal{Q}(\boldsymbol{x}[n]) \quad = \quad \mathcal{Q}\left(\boldsymbol{U}_M^\top \boldsymbol{U}_M \boldsymbol{x}[n]\right)$$

for any $\boldsymbol{x}[n] \in \mathbb{R}^M$ and $\boldsymbol{U}_M \in \mathbb{R}^{M-1 \times M}$ defined recursively as

$$\boldsymbol{U}_M = \begin{bmatrix} \sqrt{\frac{M-1}{M}} & -\sqrt{\frac{1}{M(M-1)}}\mathbf{1}_{1\times M-1} \\ \mathbf{0}_{M-2\times 1} & \boldsymbol{U}_{M-1} \end{bmatrix}$$

with

$$\boldsymbol{U}_2 = \frac{1}{\sqrt{2}}\begin{bmatrix} 1 & -1 \end{bmatrix}.$$

We note that $\boldsymbol{U}_M$ is upper triangular and $\boldsymbol{U}_M^\top \boldsymbol{U}_M = \boldsymbol{I}_M - \frac{1}{M}\mathbf{1}_{M\times M}$.

Proof: See [1] ■

It is worth considering the geometric interpretation of the projection via $\boldsymbol{U}_M$. As we noted above, a PPM signal has non-zero mean. By simple coordinate translation of a PPM signal set (i.e. by subtracting the mean from each chip), we arrive at a new signal set which is the so-called transorthogonal or simplex set [9]. Translation of the origin does not affect the Euclidean distance properties of the signal set. It is also well-known that the *dimensionality* of an M-ary simplex signal set is $M-1$ [9]; that is, through appropriate choice of coordinate system, an M-ary simplex signal set can be represented with just $M-1$ chips. Furthermore, an M-ary PPM signal set can be projected into an M-ary simplex set represented by $M-1$ chips, with identical Euclidean distance properties; this is the role of $\boldsymbol{U}_M$. Finally, we note from [1] that projection via $\boldsymbol{U}_M$

is invariant to DC offsets, so for some vector $\boldsymbol{x} \in \mathbb{R}^M$ and some scalar b,

$$\boldsymbol{U}_M(\boldsymbol{x} + b\mathbf{1}_{M\times 1}) = \boldsymbol{U}_M\boldsymbol{x}. \tag{3}$$

Thus, by building a block equalizer which outputs symbols $\tilde{\boldsymbol{x}}[n] \in \mathbb{R}^{M-1}$ of reduced dimension, it is Euclidean distance preserving, and is invariant to DC shifts at the equalizer input.

Next we make several definitions to aid our development of the equalizer coefficients. Again, in addition to the equalizer length N_f, the equalizer accepts one other design parameter, Δ, which represents the desired symbol delay through the channel/equalizer chain. By defining

$$\boldsymbol{E}_\Delta^\top \triangleq \begin{bmatrix}\mathbf{0}_{M\times M\Delta} & \boldsymbol{I}_M & \mathbf{0}_{M\times N_c-M(\Delta+1)}\end{bmatrix} \tag{4}$$

where $\boldsymbol{E}_\Delta \in \mathbb{R}^{N_c\times M}$, we can express the delayed symbol vector in terms of the source symbol stream as

$$\boldsymbol{x}[n-\Delta] = \boldsymbol{E}_\Delta^\top \bar{\boldsymbol{x}}[n]. \tag{5}$$

Our goal, then, is to choose equalizer coefficients so that $\tilde{\boldsymbol{x}}[n] \approx \boldsymbol{U}_M\boldsymbol{x}[n-\Delta]$ where we note the appearance of $\boldsymbol{U}_M$ serves to project the source signal into the space of reduced dimension so that it is compatible with the equalizer output $\tilde{\boldsymbol{x}}[n]$. Since our focus is on an equalizer with complete ISI removal, we temporarily ignore the noise, and review the conditions under which the equalizer output matches the source sequence. The ISI is eliminated if the mean square error (MSE) between the equalizer output and source signals is exactly zero in the absence of noise, or when

$$\begin{aligned} J_{mse}(\boldsymbol{\mathcal{F}},\Delta) &= E[||\tilde{\boldsymbol{x}}[n] - \boldsymbol{U}_M\boldsymbol{x}[n-\Delta]||_2^2] \\ &= 0. \end{aligned} \tag{6}$$

With the source autocorrelation for PPM given by

$$\begin{aligned} \boldsymbol{R}_{xx} &\triangleq E[\bar{\boldsymbol{x}}[n]\bar{\boldsymbol{x}}^\top[n]] \\ &= \frac{1}{M^2}\mathbf{1}_{N_c\times N_c} + \frac{1}{M}(\boldsymbol{I}_{\frac{N_c}{M}} \otimes (\boldsymbol{I}_M - \frac{1}{M}\mathbf{1}_{M\times M}). \end{aligned}$$

we define $\boldsymbol{\Phi}_{xx}^\top\boldsymbol{\Phi}_{xx} = \boldsymbol{R}_{xx}$ as the Cholesky decomposition of the source autocorrelation, where $\boldsymbol{\Phi}_{xx} \in \mathbb{R}^{N_c-N_c/M+1\times N_c}$. Letting $\boldsymbol{\mathcal{H}}' \triangleq \boldsymbol{\mathcal{H}}\boldsymbol{\Phi}_{xx}^\top$ the MSE expression reduces to [1]

$$J_{mse}(\boldsymbol{\mathcal{F}},\Delta) = \left|\left|\boldsymbol{\mathcal{F}}^\top\boldsymbol{\mathcal{H}}' - \boldsymbol{U}_M\boldsymbol{E}_\Delta^\top\boldsymbol{\Phi}_{xx}^\top\right|\right|_{fro}^2$$

where $||\cdot||_{fro}$ denotes the Frobenius norm. Thus, the condition for perfect equalization is that the MSE is zero, or

$$\boldsymbol{\mathcal{H}}'^\top\boldsymbol{\mathcal{F}} = \boldsymbol{\Phi}_{xx}\boldsymbol{E}_\Delta\boldsymbol{U}_M^\top. \tag{7}$$

For the existence of an exact solution of $\boldsymbol{\mathcal{F}}$ for this linear system, $\boldsymbol{\mathcal{H}}' \in \mathbb{R}^{N_f\times N_c-N_c/M+1}$ must be tall and full rank, leading to the following two conditions for perfect equalization:

1) *Equalizer Length Condition:* For $\boldsymbol{\mathcal{F}}$ to satisfy (7) for arbitrary Δ, $\boldsymbol{\mathcal{H}}'$ must be a tall matrix. Hence, it is required that

$$N_f > N_h(M-1) \tag{8}$$

2) *Channel Disparity Condition:* For $\boldsymbol{\mathcal{F}}$ to satisfy (7) for arbitrary Δ, $\boldsymbol{\mathcal{H}}'$ must have full column rank.

Thus, the finite-length block equalizer structure can succeed in perfectly equalizing the channel, so long as the length and disparity conditions are satisfied. In the next section we consider blind adaptation of a *scalar* chip-rate equalizer, and subsequently show how this can be used with the *block* symbol-rate equalizer described above.

III. Blind Adaptive Algorithm for PPM

A. Review of Algorithm

Recently, a globally convergent blind adaptive equalization algorithm was proposed for PPM modulations [2]. The scheme employs a chip-rate FIR equalizer $\boldsymbol{f} \in \mathbb{R}^{N_f}$ which operates on a zero-mean version of the received signal. That is, the mean of the received signal is subtracted before equalization, so that the equalizer output can be written $\tilde{x}[n] = \boldsymbol{f}^\top(\bar{\boldsymbol{y}}[n] - \mu_y\mathbf{1})$ where μ_y is the mean of the received signal. The equalizer output is then serial-to-parallel converted and fed M chips at a time into the decision device. The proposed algorithm is based on third-order moments, and adapts the equalizer coefficients to maximize the objective function

$$J(\boldsymbol{f}) = \left|E[\tilde{x}^3[n]]\right| \tag{9}$$

while constraining the norm of the equalizer taps to be 1. Intuitively, the rationale for this choice of objective function stems from the fact that a PPM signal is sparse, and is thus characterized by large skewness. Since an ISI channel serves to reduce the skewness in a PPM signal, maximizing the skewness (or third-moment) should serve to reduce the ISI in a PPM signal. It is worth pointing out that an added benefit of employing the third-moment is its insensitivity to noise [2]. As is common in the analysis of blind algorithms (e.g. [10]), the authors assume that the equalizer is sufficiently long so that the analysis can be performed in the combined channel/equalizer space $\boldsymbol{c} = \boldsymbol{\mathcal{H}}^\top\boldsymbol{f}$. In addition, however, it is assumed in [2] that the PPM alphabet size $M \to \infty$. Under these assumptions, the authors succeed in proving that the objective function exhibits maxima only at the desired equalizer settings, i.e. at zero-forcing (ZF) solutions. A corresponding steepest ascent algorithm emerges as

$$\begin{aligned} \boldsymbol{f}'[n+1] &= \boldsymbol{f}[n] + \mu\nabla_{\boldsymbol{f}}J(\boldsymbol{f}) \\ \boldsymbol{f}[n+1] &= \boldsymbol{f}'[n+1]/\sqrt{\boldsymbol{f}'^\top[n+1]\boldsymbol{f}'[n+1]} \end{aligned}$$

where the gradient in [2] is approximated by $\nabla_{\boldsymbol{f}}J(\boldsymbol{f}) \approx \mathrm{sgn}(\tilde{x}[n])\tilde{x}^2[n]\boldsymbol{y}[n]$. We note that the true gradient is $\nabla_{\boldsymbol{f}}J(\boldsymbol{f}) = \mathrm{sgn}(E[\tilde{x}^3[n]])E[\tilde{x}^2[n]\boldsymbol{y}[n]]$, and thus the chosen gradient approximation is perhaps a more accurate gradient estimate of the alternate objection function $J'(\boldsymbol{f}) = E[|\tilde{x}^3[n]|]$ since

$$\begin{aligned} \nabla_{\boldsymbol{f}}J'(\boldsymbol{f}) &= E[\mathrm{sgn}(\tilde{x}^3[n])\tilde{x}^2[n]\boldsymbol{y}[n]] \\ &= E[\mathrm{sgn}(\tilde{x}[n])\tilde{x}^2[n]\boldsymbol{y}[n]] \\ &\approx \mathrm{sgn}(\tilde{x}[n])\tilde{x}^2[n]\boldsymbol{y}[n] \end{aligned}$$

due to the fact that for a sufficiently small stepsize μ, the natural averaging inherent to stochastic gradient ascent algorithms effectively allows us to omit the *outer* expectation. Consequently, in the sequel, we employ a slightly more accurate gradient estimate for $J(\boldsymbol{f})$ yielding the update equation

$$\boldsymbol{f}[n+1] = \boldsymbol{f}[n] + \mu \cdot \operatorname{sgn}\left(\sum_m \tilde{x}^3[m]\right)\left(\sum_m \tilde{x}^2[m]\boldsymbol{y}[m]\right) \quad (10)$$

where the index m on the sums is taken over the most recent N symbols for some window size N. Nevertheless, to the best of our knowledge, this is the only known globally convergent algorithm for blind adaptation of equalizers used with PPM signals.

B. Discussion of Maxima for Finite M

While the results of [2] are very encouraging, the behavior of the algorithm for finite M is unclear. Some interesting questions might include:

- Do the desired maxima simply move away from the ZF solutions when M is finite?
- If so, how far away do they move?
- Do additional false local maxima appear for finite M?

Ideally, we would like to answer these questions analytically. However, without letting $M \to \infty$, the expression for the objective function (9) cannot readily be simplified due to the appearance of many non-zero terms in the third-order moment of the PPM signal. Nevertheless, we hope to provide some evidence that, indeed, the maxima only move slightly away from the ZF solutions, and that additional false local maxima do not seem to appear.

1) Exact locations of maxima for $N_c = 2$: For the special case where the combined channel/equalizer response $\boldsymbol{c}$ has length $N_c = 2$, we can plot the objective function and calculate the exact locations of all maxima as a function of M. To impose the constraint that the norm of the taps must be unity, we re-parameterize the 2 taps in polar coordinates, taking $c_0 = \sin\theta$ and $c_1 = \cos\theta$. We then seek the angle θ that maximizes the objective function $J(\boldsymbol{c}) = \left|E[\tilde{x}^3[n]]\right|$. Ideally, we hope that the maxima occur near the zero forcing solutions (as well as their negatives, as described in [2]), or $\boldsymbol{c} \in \{[+1,0],[-1,0],[0,-1],[0,+1]\}$, which corresponds to $\theta = n\pi/2$ for any integer n. A plot of the objective function over θ for $M = 4$ and $M = 128$ is shown in Fig. 2. As can be seen, the objective function only exhibits maxima *near* the desired ZF solutions; no additional false local maxima appear. By expanding the objective function in terms of its moments from [2], we can calculate the precise location of the maxima, and can show that they occur at

$$\theta = -\tan^{-1}\left(\frac{3 + M \pm \sqrt{M^2 + 6M + 5}}{2}\right) + n\pi$$

for any integer n. As $M \to \infty$, this expression indeed reduces to $\theta = n\pi/2$ for any integer n. Thus, for the trivial case where the combined channel/equalizer response has length 2, we have a precise expression for the distance between the true maximizers of $J(\boldsymbol{c})$ and the ZF solutions. Indeed, even for small M, the maxima are quite close to the ZF solutions. In addition, we reiterate that no additional false local maxima appear for $N_c = 2$.

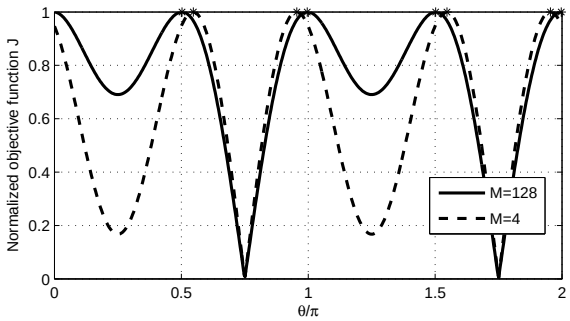

Fig. 2. Objective function for $N_c = 2$ and $M \in \{4, 128\}$

2) Numerical Investigation of Maxima for $N_c > 2$: While the results for $N_c = 2$ are encouraging, the results provide no insight into the behavior of the objective function for larger values of N_c. Unfortunately, calculating the maxima of the objective function rapidly becomes intractable even for $N_c = 3$. However, we attempt to give evidence that suggests the results for $N_c = 2$ do indeed apply for larger lengths. We proceed by conducting a numerical search over 10^{N_c-1} initializations uniformly spaced on the unit $N_c - 1$ sphere, and employ the uphill simplex method [11] in attempt to characterize all maxima of the objective function. Note that we again need to re-parameterize the cost function in polar coordinates so that the unit norm constrain is imposed. For a given N_c, we require $N_c - 1$ angles θ_i for $i = 0, \ldots, N_c - 2$, and the chosen parameterization is given by:

$$c_i = \begin{cases} \sin\theta_i \prod_{j=0}^{i-1} \cos\theta_j & 0 \le i \le N_c - 3 \\ \prod_{j=0}^{N_c-2} \cos\theta_j & i = N_c - 2 \end{cases}.$$

For each of the 10^{N_c-1} initializations and their corresponding maxima, we calculate the Euclidean distance of each maxima from its nearest ZF solution (including negated ZF solutions). As the number of initalizations to consider grows exponentially with the number of channel/equalizer taps, we are only able to search the range $2 \le N_c \le 6$. The results are shown in Fig. 3, where we see that the maxima for finite M are *very* close to ZF solutions in general. Again, for this numerical search, the only maxima appear to be near ZF solutions; no additional local maxima were found. We also note that as $M \to \infty$, the locations of the maxima do indeed approach the ZF solutions as reported in [2]. While this exercise is certainly not a definitive proof, it does suggest that the objective function may only exhibit "good" maxima that are very near the desired ZF solutions even for finite M. In addition, we note that all of the convergent values in this experiment correspond to "open-eye" solutions where the decision device makes no errors in the absence of noise.

IV. Switching from Scalar to Block Equalizer

We now investigate use of the algorithm (10) for cold startup of the scalar chip-rate equalizer, followed by switching

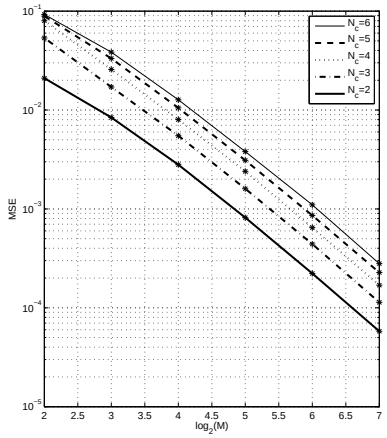

Fig. 3. Proximity of maxima to ZF solutions as a function of M

to the block symbol-rate equalizer of section II which can subsequently be adapted with decision-directed least mean squares (DD-LMS). It is well known that DD-LMS is not a good choice for cold-startup from initializations which are not open-eye. With the recent discovery of a suitable algorithm for cold-startup of a scalar equalizer [2] (and our results from section III which suggest that it always converges near a ZF solution for finite M), we expect that this algorithm can be used for cold-startup of the block equalizer.

Recall that for the blind algorithm (10), the equalizer output for a single chip of the M-PPM signal can be written $\tilde{x}[n] = \boldsymbol{f}^\top(\bar{\boldsymbol{y}}[n] - \mu_y \mathbf{1})$. Equivalently, we could write an entire equalized symbol as $\boldsymbol{\mathcal{F}}_*^\top(\bar{\boldsymbol{y}}[n] - \mu_y \mathbf{1})$ where

$$\boldsymbol{\mathcal{F}}_* = \begin{bmatrix} \boldsymbol{f} & 0 & \cdots & 0 \\ 0 & \boldsymbol{f} & & \vdots \\ & \ddots & & 0 \\ & & & \boldsymbol{f} \end{bmatrix} \in \mathbb{R}^{N_f+M-1 \times M}. \tag{11}$$

Projecting the equalized result into the relevant $M-1$ dimensional subspace gives:

$$\begin{aligned} \tilde{\boldsymbol{x}}[n] &= \boldsymbol{U}_M \boldsymbol{\mathcal{F}}_*^\top (\bar{\boldsymbol{y}}[n] - \mu_y \mathbf{1}) \\ &= \underbrace{\boldsymbol{U}_M \boldsymbol{\mathcal{F}}_*^\top}_{\triangleq \boldsymbol{\mathcal{F}}_{init}^\top} \bar{\boldsymbol{y}}[n] \end{aligned}$$

where we use the fact that $\boldsymbol{U}_M \boldsymbol{\mathcal{F}}_*^\top \mathbf{1} = \mathbf{0}$ which follows from (3). A candidate cold startup-scheme for M-PPM then emerges:

1) Adapt a scalar chip-rate equalizer $\boldsymbol{f}$ using (10).
2) After sufficient number of iterations, some form of symbol synchronization (i.e. identification of symbol boundaries) needs to be performed. This amounts to an M-ary hypothesis testing problem which could be solved by choosing the symbol boundary so that all symbols to have roughly equal power.
3) We then switch to using the block symbol-rate equalizer with the equalizer coefficients set to $\boldsymbol{\mathcal{F}} = \boldsymbol{\mathcal{F}}_* \boldsymbol{U}_M^\top$ where $\boldsymbol{\mathcal{F}}_*$ is defined in (11).
4) Adaptation of the block equalizer can then proceed using DD-LMS via

$$\boldsymbol{\mathcal{F}}[n+1] = \boldsymbol{\mathcal{F}}[n] - \mu \bar{\boldsymbol{y}}[n](\tilde{\boldsymbol{x}}[n] - \boldsymbol{U}_M \hat{\boldsymbol{x}}[n])^\top$$

where μ is a small positive step-size which serves to average out the noise in the gradient estimate.

V. Numerical Results and Conclusion

A simulation was conducted using 4-PPM transmission over 1000 randomly generated Rayleigh WSSUS channels with length $N_h = 10$ and 10 dB SNR. The equalizer length was chosen to be $N_f = 30$. The startup procedure outlined above was employed, where the blind algorithm in step 1 was given 1000 PPM symbols before switching to the decision-directed block equalizer. We note that DD-LMS will in general converge to the MMSE equalizer solution, and not the ZF solution. Nevertheless, for each of the 1000 channel realizations, we observed the ability of the cold startup scheme to sufficiently open the eye so that there would be no errors if the noise were removed. As hoped, the equalizer succeeded in opening the eye for all 1000 realizations, suggesting that indeed the cold startup procedure is a good candidate for use with the block equalizer structure.

We have presented a cold-startup strategy which combines the techniques presented in [1] and [2], and seems to be a promising choice for blind equalization of PPM signals. Future work could characterize (or bound) the exact locations of the maxima of (9), and show that they lie in the regions of convergence for DD-LMS, thus providing more analytical evidence in support of this cold-startup strategy.

References

[1] A. Klein and P. Duhamel, "Decision-feedback equalization for pulse-position modulation," *IEEE Trans. Signal Process.*, vol. 55, pp. 5361–5369, Nov. 2007.

[2] P. Pääjärvi, "Blind equalization using third-order moments," Ph.D. dissertation, Lulea tekniska universitet, Sweden, May 2008. [Online]. Available: http://pure.ltu.se/ws/fbspretrieve/1918433

[3] M. Audeh, J. Kahn, and J. Barry, "Decision-feedback equalization of pulse-position modulation on measured nondirected indoor infrared channels," *IEEE Trans. Commun.*, vol. 47, pp. 500–503, Apr. 1999.

[4] M. Z. Win and R. A. Scholtz, "Ultra-wide bandwidth time-hopping spread-spectrum impulse radio for wireless multiple-access communications," *IEEE Trans. Commun.*, vol. 48, pp. 679–689, Apr. 2000.

[5] J. Barry, "Sequence Detection and Equalization for Pulse-Position Modulation," in *Proc. IEEE International Conference on Communications (ICC'94)*, May 1994, pp. 1561–1565.

[6] C. Carbonelli and U. Mengali, "M-PPM noncoherent receivers for UWB applications," *IEEE Trans. Wireless Commun.*, vol. 5, p. 22852294, Aug. 2006.

[7] M. Audeh, J. Kahn, and J. Barry, "Performance of pulse-position modulation on measured non-directed indoor infrared channels," *IEEE Trans. Commun.*, vol. 44, pp. 654–659, Jun. 1996.

[8] L. Tong, G. Xu, and T. Kailaith, "Fast blind equalization via antenna arrays," in *Proc. IEEE Intl. Conf. on Acoustics, Speech, and Signal Processing (ICASSP'93)*, Apr. 1993, pp. 272–275.

[9] J. Proakis, *Digital Communications*, 4th ed. New York: McGraw-Hill, 2000.

[10] G. Foschini, "Equalizing without altering or detecting data," *Bell Sys. Tech. J.*, vol. 64, pp. 1885–1911, Oct. 1985.

[11] M. Avriel, *Nonlinear Programming: Analysis and Methods*. Dover Publishing, 2003.